Environ. Sci. Technol. **1999**, *33,* 1819−1824

Mineralization of Sparsely Water-Soluble Polycyclic Aromatic Hydrocarbons in a Water Table Fluctuation Zone

H.-Y. N. HOLMAN,* Y. W. TSANG, AND W. R. HOLMAN†

Lawrence Berkeley National Laboratory, University of California, Berkeley, California 94720

The mineralization potential of sparsely water-soluble polycyclic aromatic hydrocarbons (PAHs) within a highly diesel-contaminated water table fluctuation zone (WTFZ) was investigated using core-scale column microcosms. Experimental conditions mimicked overall seasonal changes in water and oxygen content at the site. During the first aerobic winter, PAH mineralization rates in the freshly contaminated soil were fastest for contaminant [^{14}C]-naphthalene which was the least hydrophobic and most water-soluble. Lowering the water table nearly doubled the mineralization rates of all [^{14}C]PAHs studied. During the oxygen-poor summer, all mineralization rates were insignificant and failed to respond to water table changes. Neither a return to water-saturated aerobic (winter) conditions nor lowering the water table under aerobic conditions induced detectable mineralization of [^{14}C]-naphthalene, but lowering the water table did markedly hasten the still slow mineralization of [^{14}C]phenanthrene and [^{14}C]anthracene. The time-dependent mineralization behavior and its response to water table fluctuations were explicable in terms of microbial responses to the changing oxygen content and depleting mineral nutrients.

Introduction

Petroleum products released from leaking storage facilities can reach the capillary fringe and are often trapped within the water table fluctuation zone (WTFZ) (*1*). These trapped petroleum products include polycyclic aromatic hydrocarbons (PAHs). Their low volatility and water solubility allow them to persist in subsurface environments. Their mineralization to harmless CO_2 and H_2O by intrinsic microorganisms is believed to be the major process removing them from soils. It has been the focus of many studies (*2*−*21*), but few of these incorporated oscillating conditions akin to those within a WTFZ.

The rise and fall of a water table is a common subsurface phenomenon that can affect key environmental parameters (*22*−*24*), microbial populations, and their biological activities (*25*−*30*). If the WTFZ is contaminated with trapped petroleum hydrocarbons, a fluctuating water table can also influence the availability of the associated sparsely water-soluble PAHs to microorganisms (*31*) and their subsequent metabolic transformation (*32*). This paper reports a laboratory investigation of PAH mineralization following a diesel spill that reached a WTFZ. The objective was to examine the changing mineralization behavior of PAHs with protracted resident time in a water table fluctuating environment that was heavily contaminated with diesel oil.

This investigation used core-scale column microcosms designed specifically to mimic the changes in water saturation and oxygen content which accompany seasonal changes in a WTFZ at a central California site. Exemplar sparsely water-soluble PAHs were naphthalene, phenanthrene, and anthracene, in order of descending solubility (31, 1.10, and 0.045 g/m^3) (*33*) and ascending hydrophobicity (as represented by their equilibrium partition coefficients (log K_p) of 2.91, 3.22, and 3.34). The progress of PAH mineralization was monitored by radiorespirometry, which presumes that microorganisms degrade both radiolabeled and nonlabeled PAHs in a similar manner.

Experimental Section

Site Description. The WTFZ was in a 30-year old diesel-contaminated area within a hill near San Francisco. It contained disconnected centimeter-scale bands of diesel oil. Central California's wet winters and dry summers impart a seasonal alternation between two distinct redox states in this low-permeability WTFZ. Aerobic conditions accompany the infiltration of oxygenated rainwater and entrained air during winter, whereas oxygen-poor conditions accompany summer. The oxygen-poor conditions of summer arise from microbial consumption of oxygen that exceeds the rate of air replenishment in this low-permeability silt loam.

Soil Characteristics. Pristine soil cores and groundwater samples were collected in an argon atmosphere. Soil cores were from a depth of 2.5−3.0 m within the WTFZ. Table 1 lists the relevant biological, chemical, mineral, and physical properties of the pristine soil.

Radiochemicals. The mineralization of naphthalene, phenanthrene, and anthracene were quantified using high-purity [1-^{14}C]naphthalene, [9-^{14}C]phenanthrene (from the Sigma Chemical Co. of St. Louis, MO), and [side ring-^{14}C]-anthracene (from Amersham Corporation of the United Kingdom). The purity of all [^{14}C]PAHs was checked by radiochemical GC/FID and HPLC and found to be at least 99% pure. Thus, production of $^{14}CO_2$ exceeding 1% clearly represents [^{14}C]PAH mineralization. A nanomolar concentration of a single [^{14}C]PAH was mixed into filter-sterilized diesel oil and then added to its own batch of experimental soil. The resulting radioactivity levels were approximately 10^6 dpm/mL of diesel oil.

Preparation of Soil. Soil samples were aseptically mixed, air dried, and passed through a 2.0-mm sieve in a laminar flow hood. The soil was acclimated with hydrocarbon-degrading microorganisms that typify highly contaminated soils by mixing 3.5 mL of filter-sterilized nonlabeled diesel oil into each 100 g of soil, followed by incubation at 21 ± 1 °C in the dark for three weeks. Acridine orange (AO) direct counts (in triplicate) showed that microorganisms increased from $3.1 \times 10^6 \pm 1.1 \times 10^6$ to $8.6 \times 10^6 \pm 0.4 \times 10^6$ microorganisms/g of oven-dry soil in the first 2 weeks but changed little thereafter. The soil to be used in the abiotic microcosms was then irradiated overnight by a 6000-Ci ^{60}Co source over three consecutive nights. Irradiation introduced no detectable changes in the physical and chemical properties of the soil. Standard plate counts detected no colony forming units. We attributed any $^{14}CO_2$ produced in these microcosms to abiotic processes.

* Corresponding author phone: (510)486-5943; fax: (510)486-7152; e-mail: hyholman@lbl.gov.

† Present address: MS:70A-3317, Center for Environmental Biotechnology, Lawrence Berkeley National Laboratory, University of California, Berkeley, CA 94720.

10.1021/es980701k CCC: $18.00
Published on Web 04/15/1999

TABLE 1. Physical, Chemical, and Biological Characteristics of the Silt Loam Used in This Study

soil texture (% by wt of oven-dry soil)	
clay:sand:silt	18:34:48
USDA texture	silt loam
pH − paste (units)	7.9
cation-exchange capacity (meg/kg)	111
total organic carbons (%)	0.2
total nitrogen (%)	1.8
nitrate nitrogen (ppm)	55.2
organic nitrogen (%)	1.8
ammonia (%)	<0.001
phosphate (ppm)	17.1
maximum water retention capacity (%)	44.6
water-content/water-potential relationship[a]	
air-dry; 30; 50; 70%	≤−10.0; −0.5; −0.025; ≥−0.01 MPa
PAH equilibrium partition coefficient	(log K_p)
naphthalene	2.91
phenanthrene	3.22
anthracene	3.34
bacteria population	
AO direct count (microorganisms/g)	$3.1 \times 10^6 \pm 1.1 \times 10^6$
no. of heterotrophs in soils (cfu/g)	$2.7 \times 10^6 \pm 0.2 \times 10^6$

[a] Obtained by slowly drying the water-saturated silt loam.

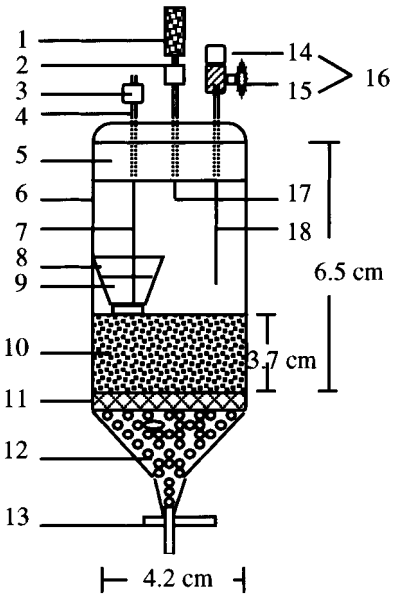

FIGURE 1. Schematic of a column microcosm: (1) ascarite $^{14}CO_2$ absorbent trap; (2) one-way air-exchange port; (3) sampling port; (4) hypodermic needle; (5) stopper; (6) Buchner funnel; (7) capillary Teflon tubing; (8) 5-mL ceramic cup; (9) 2 N NaOH solution; (10) 50 g of soil; (11) fritted bottom disc; (12) sterile glass beads; (13) three-way water influent port; (14) inlet no. 2; (15) inlet no. 1 with 0.2-μ filter; (16) three-way air-echange port; and (17) and (18) capillary Teflon tubing.

Preparation of Column Microcosms. Figure 1 depicts schematically the column microcosm. All components used in constructing the column microcosms were autoclaved at 120 °C and 18 psi for 20 min and assembled inside a laminar flow hood. All tubing and valves were made of Teflon, stainless steel, or glass. Its main section was a Pyrex Buchner funnel with a fritted bottom disc of medium porosity. The microcosm was flooded or drained through the influent port. The 2 N NaOH solution was used to trap $^{14}CO_2$ generated during the experiment. The 20−30-mesh ascarite was used to trap $^{14}CO_2$ from the air forced out when the water level in the microcosm was raised. The amount of $^{14}CO_2$ trapped by the ascarite was measured by the degassing technique described in ref *17*. Inlet no. 1 of the three-way air-exchange valves allowed the O_2 concentration in the microcosm atmosphere to be monitored while providing for air-exchange (with ambient air) as the water level changed. The on-line 0.2 μm filter at inlet no. 2 was to filter-sterilize incoming ambient air. We used a layering-and-vibration technique similar to that described in *34* to pack 50 g of the PAH-enriched soil into each funnel under water saturated conditions. Soil water was drained at the completion of the packing process.

Experimental Procedure. One abiotic and two biotic column microcosm experiments were conducted for each of the three representative PAHs. Each experiment began with an injection of 0.3 mL of the filter-sterilized [^{14}C]PAH-containing diesel oil into the bottom of the soil column. A stopper sealed the funnel immediately afterward. To sorb [^{14}C]PAHs throughout the soil column (and thereby mimic a band of trapped diesel oil within the WTFZ), the water level was raised to the soil surface and then lowered and raised three times at a rate of 0.25 cm/min. The final concentration of diesel oil was 3.2% (by weight). Concentrations of the unlabeled two-ring and three-ring PAHs were 130 and 360 ppm, respectively. All column microcosms were then incubated in the dark at room temperature (21 ± 1 °C) for 390 days.

A parallel nonlabeled microcosm experiment assessed the changing microbial population density through acridine orange (AO) direct counts. Near the end of the experiment, an additional nutrient analysis for nitrate-nitrogen and phosphate in the soil was conducted.

Experimental Conditions. Our choice of experimental conditions was based on observations that the ground water table at this site did not respond immediately to individual storms because of the low permeability and other hydrogeologic conditions. Depending on storm frequency and intensity, the winter can be treated as a single cycle of flood and drain. The water table remained fairly stable throughout the dry summer. We imposed a summer flood-and-drain simply for the purpose of comparisons.

Figure 2 shows the experimental conditions we used to mimic the seasonal alternation between the two distinct water and oxygen content regimes at the site. The water content of the drained soil columns averaged 40%, which is within the optimum moisture range for the microbial activity in this silt loam (*35*). The aerobic phase in this figure simulated the first aerobic "winter". Columns were initially saturated with oxygenated groundwater. Aerobic conditions were maintained by replacing all air in the column headspace with the filter-sterilized ambient air after each $^{14}CO_2$ sample

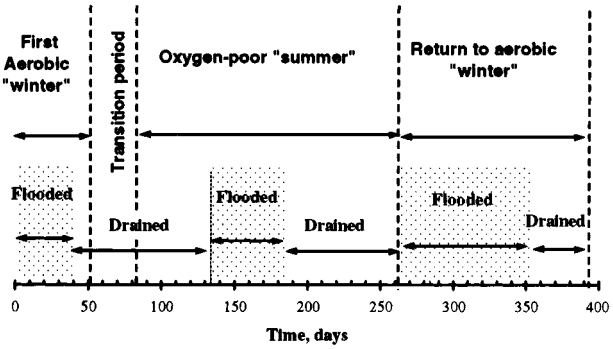

FIGURE 2. A schematic diagram of experimental conditions used in this study. To mimic changing water and oxygen contents, each microcosm experienced a sequence of aerobic, then oxygen-poor, and then once again aerobic conditions in concert with water table changes. The aerobic phase simulated the first aerobic "winter", the oxygen-poor ($O_2 \leq 1\%$) phase dry summers.

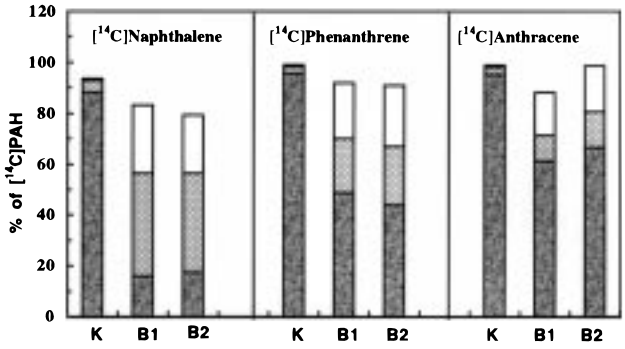

FIGURE 3. Mass balance analysis of the distribution of $^{14}CO_2$ (□), [^{14}C]PAHs (grey box), and water-soluble metabolites (box filled with dots) in the abiotic and biotic microcosms at the end of the experiment: K = killed, B1 = biotic, and B2 = biotic duplicate.

collection. The cumulative losses of $^{14}CO_2$ and [^{14}C]PAHs by this replenishment process were estimated by passing the effluent sequentially through six narrow 6-cm long vials. The first three vials were filled with 2 N NaOH solution to trap the escaped $^{14}CO_2$; the last three were filled with butanol to trap the [^{14}C]PAH vapor. Radioactivity of the trapped $^{14}CO_2$ and the [^{14}C]PAH vapor was measured using the LKB WALLAC 1219 RACKBETA liquid scintillation counter (LSC). Estimates of cumulative loss derived from these empirical measurements were less than 5% for $^{14}CO_2$, 10% for [^{14}C]naphthalene, and much less for the other [^{14}C]PAHs.

The oxygen-poor ($O_2 \leq 1\%$) phase in Figure 2 simulated dry summers. For the biotic microcosms, a low oxygen content in the headspace and pore water resulted from microbial metabolic activities that deplete the oxygen available in the microcosm. For abiotic microcosms, the atmosphere was simply replaced with a filter-sterilized oxygen-free gas mixture (80% N_2 and 20% CO_2). The pore water in the abiotic microcosms was replaced with degassed and sterilized groundwater. Saturating the entire silt loam column with oxygenated groundwater and filling the headspace with filter-sterilized air restored the microcosms to aerobic winter conditions.

Production of $^{14}CO_2$ during the experiment was monitored by periodically retrieving the NaOH solution and measuring its radioactivity. The trapping efficiency of $^{14}CO_2$ (defined as the fraction of $^{14}CO_2$ that was absorbed by the 2 N NaOH solution) was measured to be 91% by a technique similar to that described in refs *17* and *35*. All $^{14}CO_2$ values reported in this paper were adjusted upward to correct for this $^{14}CO_2$ collection efficiency.

Mineralization Pattern Analysis. The mineralization pattern of the individual [^{14}C]PAHs was estimated according to the method described in ref *36*. The pattern included the lag phase (days), mineralization period (days), percentage mineralized, maximum mineralization rate (%/day), and overall mineralization rate (%/day).

Mass Balance Assay. At the end of the column microcosm experiment, a gram of the well-mixed experimental soil was removed from each microcosm that had [^{14}C]PAHs. The soil was sonicated for 20 min in a mixture of 5 mL of ethyl acetate and 10 mL of water. The [^{14}C]PAHs and their [^{14}C]metabolites in the disrupted soil particles were extracted in the ethyl acetate/water mixture in multiple overnight extractions. We used the extraction method described in ref *21* until radioactivity in the extract had declined to the instrument background (40 dpm). LSC measurements of radioactivity of [^{14}C]PAHs in ethyl acetate and of [^{14}C]metabolites in water were corrected for the "quenching effects" of soil materials using the internal-standard technique of Gatti (*37*). The technique involved measuring the initial radioactivity R_i of the sample, spiking the sample with the corresponding ^{14}C-labeled PAHs of known radioactivity R_s, and then measuring the total radioactivity R_t of the spiked sample. The actual radioactivity of the sample was calculated from $R_i \times R_s/(R_t - R_i)$.

The amount of [^{14}C]PAHs and their byproducts in experimental groundwater that was collected during various phases of the experiment was measured analogously.

Oxygen Measurements. O_2 concentrations within the headspace of the column microcosms were monitored by an OM-4 Oxygen Meter [Microelectrodes, Inc., Bedford, NH] equipped with a flow through oxygen microprobe. It was calibrated with pure nitrogen gas (0% O_2) and air (20.9% O_2). The concentration of O_2 dissolved in the groundwater was measured by a dissolved oxygen meter [Hachi Model 16046]. The meter was calibrated with deionized water that had been purged at the water boiling point for 20 min with pure nitrogen (0 ppm dissolved O_2) and with water purged with pure O_2 at 21 °C (8.7 ppm dissolved O_2).

Results

Mineralization of [^{14}C]PAHs in Killed Controls. The $^{14}CO_2$ evolved in the absence of metabolically active microorganisms totaled about 1% of the [^{14}C]PAHs available. This was insufficient to demonstrate abiotic mineralization of [^{14}C]-PAHs, because impurities comprised about 1% of the [^{14}C]-PAHs. An ethyl acetate/water extraction mass balance assay (Figure 3) showed that 88% of the [^{14}C]naphthalene and more than 95% of the [^{14}C]phenanthrene and [^{14}C]anthracene were ethyl acetate-extractable [^{14}C]compounds. Only 5% of the [^{14}C]naphthalene and 3% of the [^{14}C]phenanthrene and [^{14}C]-anthracene had been converted to water-extractable polar byproducts.

Mineralization of [^{14}C]PAHs in Biologically Active Column Microcosms. Figure 4 depicts the cumulative evolution of $^{14}CO_2$ during the experimental sequence of aerobic, then oxygen-poor, and then aerobic conditions, each accompanied by a water table fluctuation. Mineralization rates are summarized in Table 2. Microbial production of $^{14}CO_2$ was the greatest in freshly contaminated soil during the first aerobic "winter" but only after an initial lag period. Mineralization of [^{14}C]naphthalene, the least hydrophobic and most water-soluble of the three PAHs, proceeded slowly for two days (see insert in Figure 4) and then accelerated rapidly. Mineralization of the less water-soluble and more hydrophobic [^{14}C]phenanthrene and [^{14}C]anthracene proceeded very slowly for four and five days, respectively, before acceleration began. These lag times are within the range of those reported elsewhere for soil microcosms (*2*, *17*, *35*, *39*, *40*).

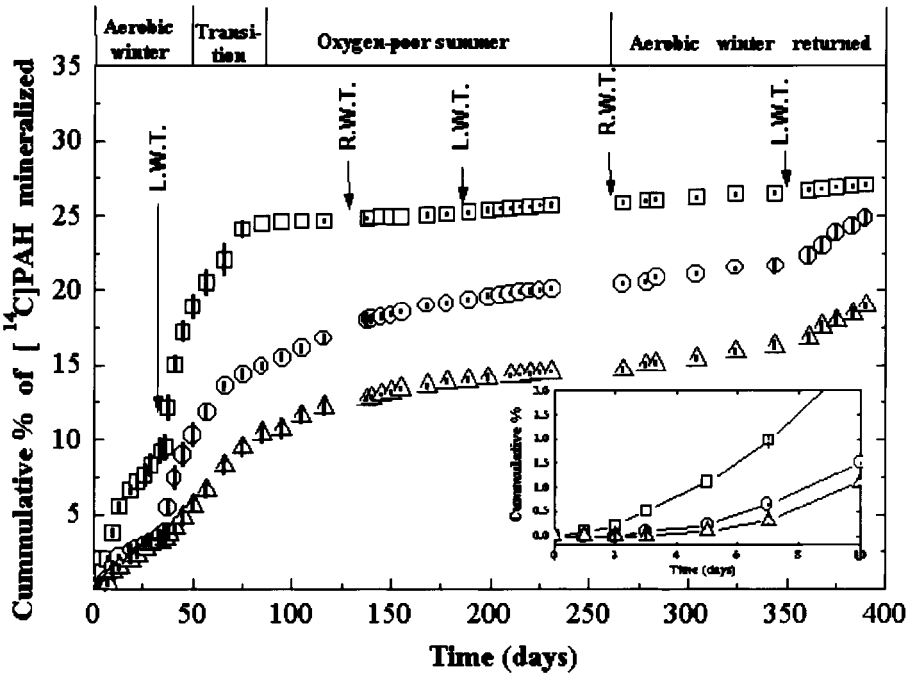

FIGURE 4. Measured cumulative production of $^{14}CO_2$ from [1-^{14}C]naphthalene (□), [9-^{14}C]phenanthrene (○), and [*side ring*-^{14}C]anthracene (△) (LWT = lowered water table and RWR = raised water table).

TABLE 2. Summary of the Measured Mineralization Rates

	first aerobic "winter season"							return to aerobic "winter season"		
		with wtf[a]				oxygen-poor "summer season"		with wtf[a] (%/day)		
[^{14}C]PAHs	lag phase (day)	max. (%/day)	av (%/day)	without wtf[a,b] (%/day)	transition (%/day)	with wtf[a] (%/day)	without wtf[a,b] (%/day)	max. (%/day)	av (%/day)	without wtf[a,b] (%/day)
naphthalene	2	0.77	0.38	0.20	0.20	0.000	0.0000.000	0.000	0.000	
phenanthrene	4	0.46	0.22	0.08	0.16	0.027	0.027	0.062	0.035	0.012
anthracene	5	0.18	0.12	0.06	0.16	0.020	0.013	0.057	0.033	0.012

[a] wtf = water table fluctuations. [b] Estimated asymptotically.

By day 12, 5.5% of the [^{14}C]naphthalene, 3% of the [^{14}C]-phenanthrene, and 2% of the [^{14}C]anthracene had been mineralized. [^{14}C]naphthalene's shorter lag phase and faster mineralization rate in freshly contaminated soil have been noted elsewhere (*13*, *39*, *40*). Mineralization rates declined almost 82% after day 12. A distinct slowing after a rapid initial mineralization has been noted elsewhere in the literature (*2*, *17*, *35*, *39*, *40*).

The water table was lowered on day 37. Between day 37 and day 50, an additional 10% of the [^{14}C]naphthalene, 6% of the [^{14}C]phenanthrene, and 2.4% of the [^{14}C]anthracene were mineralized. Mineralization rates rose substantially. They averaged 0.77%/day for [^{14}C]naphthalene, 0.46%/day for [^{14}C]phenanthrene, and 0.18%/day for [^{14}C]anthracene. These rates are comparable to those reported for soil samples in batch reactors under aerobic conditions (*5*, *12*−*14*, *35*).

By the end of the first aerobic "winter", a total of 19% of the [^{14}C]naphthalene, 11% of the [^{14}C]phenanthrene, and 6% of the [^{14}C]anthracene had been mineralized. Had the soil remained saturated throughout this "season", the cumulative percentage of [^{14}C]PAHs mineralized would have asymptotically approached only 10%, 4%, and 3%, respectively. Exposing freshly contaminated silt loam to ambient air by lowering the water table roughly doubled the overall mineralization rates of all [^{14}C]PAHs.

During the transition to the subsequent oxygen-poor "summer", microbial metabolism depleted the headspace oxygen concentration from 20.9% on day 50 to less than 4% on day 80. $^{14}CO_2$ production slowed concurrently. Only 6% of the original [^{14}C]naphthalene and 5% of [^{14}C]phenanthrene and [^{14}C]anthracene were mineralized during the transition period. By day 80, mineralization rates had declined by 83% for [^{14}C]naphthalene, 72% for [^{14}C]phenanthrene, but only 11% for [^{14}C]anthracene.

The subsequent oxygen-poor "summer" lasted for 180 days. The mean O_2 concentrations in the headspace of column microcosms decreased from 5% on day 80 to below the detection limit (1%) after day 130. "Summer" mineralization totaled less than 1% for [^{14}C]naphthalene, 5% (0.027%/day) for [^{14}C]phenanthrene, and 3.5% (0.020%/day) for anthracene. These mineralization rates are more than an order of magnitude slower than the maximum mineralization rates measured during the first aerobic "winter". They are also up to an order of magnitude less than the rates of anaerobic mineralization reported elsewhere (*9*−*11*). A water table fluctuation had no discernable effect on the production of $^{14}CO_2$.

Mineralization rates failed to rebound with the onset of the next aerobic winter on day 260. Instead, they remained similar to those measured during the preceding oxygen-poor summer "season". Between day 260 and day 350, less than 1% of the [^{14}C]naphthalene and only 2% (0.022%/day) of the [^{14}C]phenanthrene and [^{14}C]anthracene were converted to $^{14}CO_2$. On day 350, the water level was lowered, and the pore water displaced by air. The effect on mineralization of [1-^{14}C]-naphthalene was negligible, but mineralization of [9-^{14}C]-

phenanthrene and [side ring-^{14}C]anthracene accelerated more than 3-fold. Between day 350 and day 390, a further 2.5% of the original [^{14}C]phenanthrene and 2.3% of the [side ring-^{14}C]anthracene were mineralized. Nonetheless, overall mineralization rates during the second "winter" were only 1/6 and 1/4 of the rates measured for [^{14}C]phenanthrene and [side ring-^{14}C]anthracene over the first "winter".

A mass balance analysis indicated that amost of the [^{14}C]-PAHs and their polar [^{14}C]metabolites remained in the soil at the end of the study (Figure 3). Their distribution in the soil is compound-dependent. Only 20% of the [1-^{14}C]-naphthalene remained, while another 40% had been converted to water-extractable metabolites. In contrast, more than half of the [9-^{14}C]phenanthrene and [side ring-^{14}C]-anthracene remained, and less than 20% was converted.

Microbial Observations in Non-[^{14}C]labeled Column Microcosm. The microbial population density remained surprisingly steady for the first 120 days (i.e., up to the first 40 days of the oxygen-poor "summer"). It ranged from $7.2 \times 10^6 \pm 0.1 \times 10^6$ to $8.5 \times 10^6 \pm 0.3 \times 10^6$ microorganisms/g,which is slightly less than the initial population density. The density value then decreased rapidly to $1.9 \times 10^5 \pm 0.7 \times 10^5$ microorganisms/g by the end of the oxygen-poor "summer"; it did not recover thereafter. A nutrient analysis indicated that the concentration of nitrate-nitrogen had decreased from the initial 55.6 to 0.1 ppm by the end of the experiment, and phosphate had been entirely depleted.

Discussion

Mineralization of [^{14}C]PAHs in Killed Controls. Abiotic production of $^{14}CO_2$ from [^{14}C]PAHs was insignificant, as in our earlier study (*35*). Although we identified neither the ethyl acetate- nor the water-extractable compounds, most of the ethyl acetate-extractable compounds are probably the original [^{14}C]PAHs, not the polymerized [^{14}C]PAHs of higher molecular weight that have been observed in dry soils and reported in (*21*). The high soil moisture content (≥12%) in our microcosm experiments discouraged such polymerization. The small quantities of [^{14}C]metabolites are probably the byproducts of oxidation processes similar to those that took place on soil mineral surfaces (*41*).

Mineralization of [^{14}C]PAHs in Biologically Active Column Microcosms. During the first "winter", lag times were observed for all [^{14}C]PAHs (see insert in Figure 4). The reasons for the observed lag phase are unclear, but various reasons have been reported (*6*, *42*−*45*).

During the post-lag period (up to day 12), the more rapid mineralization of [^{14}C]naphthalene over [^{14}C]phenanthrene and [^{14}C]anthracene was possibly due to naphthalene's higher solubility (and less hydrophobicity in this case). As has been observed in other mineralization studies (*5*, *13*−*14*), a higher solubility increases the susceptibility of individual [^{14}C]PAHs to its initial microbial attack.

We attributed most of the slowing of mineralization rates after day 12 to the depletion of dissolved oxygen, the availability of which was limited by oxygen diffusion. Oxygen's low solubility profoundly limited its transport through water-saturated pore-space to microbial concentrations in the soil mesopore (*46*, *47*). Draining the soil on day 37 filled most of its pore-space with air, creating much shorter diffusion paths and a much larger air−water interface. This greatly facilitated oxygen transport to microbes, raised their biological activities, and accelerated mineralization rates.

The more selective steep decline in the mineralization of both [^{14}C]naphthalene and [^{14}C]phenanthrene during the transition from the first aerobic "winter" to the subsequent oxygen-poor "summer" implied that the metabolic activities of [^{14}C]naphthalene-degraders in our silt loam were more sensitive to the oxygen and nutrient deprived conditions (as discussed below) than those of [^{14}C]anthracene-degraders. Similar observations have been reported for other soil systems (*19*, *39*).

The insignificant $^{14}CO_2$ production during the subsequent anaerobic "summer" could result from the very limited ability of our microorganisms to utilize [^{14}C]PAHs as a carbon and energy source. That conversion of [^{14}C]naphthalene to $^{14}CO_2$ essentially ceased under the oxygen-poor conditions indicates that few [^{14}C]naphthalene-degraders could mineralize [^{14}C]naphthalene under combined anoxic and nutrient deprived conditions. Nitrate nitrogen and phosphate had been depleted completely by the end of every biotic experiment. Although we did not analyze for soil nutrients until then, it is possible that the soils had been depleted of nutrients even earlier, as indicated by the drastic decline in viable microbial populations by late summer. Extreme nutrient deficiency is common amidst high concentrations of petroleum hydrocarbons (*1*, *48*). Petroleum products (particularly diesel oil) provide microorganisms with an imbalance food source too rich in carbon. Since biomass contains more than carbon (e.g., $C_{106}N_{16}P$), the metabolism of petroleum under high carbons and low nutrient can cause an elemental imbalance in biomass. This inhibits protein synthesis and suppresses the catabolic processes and enzymatic activities responsible for PAH transformation (*48*).

Nutrient deficiency, the persistence of [^{14}C]phenanthrene and [^{14}C]anthracene, and the accumulation of [^{14}C]metabolites imply that metabolic inhibition slowed $^{14}CO_2$ production from these two [^{14}C]PAH compounds after the onset of the second winter. Nutrient deprived naphthalene-degraders do die more quickly under anoxic than oxic conditions (*49*). This may explain the failure to mineralize [^{14}C]naphthalene when aerobic conditions returned after a long period of anoxic and nutrient deprived conditions.

This study is a first step toward understanding the intrinsic mineralization behavior of sparsely water-soluble PAHs in a WTFZ that is heavily contaminated with diesels. Our core-scale laboratory measurements show that despite the oxygen introduced by a fluctuating water table, mineralization rates decreased after a time because of nutrient deprivation. Intrinsic mineralization of PAHs in soils contaminated with high concentrations of diesel oil will slow down after an initial burst of metabolic activity if soil mineral nutrients are readily depleted. Even under optimal oxygen and moisture conditions, microbial degradation may cease unless one augments the supply of rate-limiting nutrients.

The authors thank Drs. Jennie C. Hunter-Cevera and Will T. Stringfellow and the reviewers for their helpful comments and discussions. This work was partly supported by the Laboratory Director Research Development Funds at the Lawrence Berkeley National Laboratory, University of California, under U.S. Department of Energy Contract No. DE-AC03-76SF00098.

Literature Cited

(1) Smoley, C. K. *Bioremediation of Petroleum Contaminated Sites*; CRC Press, 1992; Chapters 1−2.
(2) Carriere, P. P. E.; Mesania, F. A. Waste Management **1996**, *15*, 579.
(3) Leduc, R.; Samson, R.; Al-Bashir, B.; Al-Hawari, J.; Cseh, T. *Water Sci. Technol.* **1992**, *26*, 51.
(4) Guerin, W. F.; Boyd, S. A. *Water Res.* **1997**, *31*, 1504.
(5) Carmichael, L. M.; Christman, R. F.; Pfaender, F. K. *Environ. Sci. Technol.* **1997**, *31*, 126.
(6) Carmichael, L. M.; Pfaender, F. K. *Biodegradation* **1997**, *8*, 1.
(7) Carmichael, L. M.; Pfaender, F. K. *Environ. Toxicol. Chem.* **1997**, *16*, 666.
(8) Herbes, S. E.; Schwall, L. R. *Appl. Environ. Microbiol.* **1978**, *35*, 306.
(9) Coates, J. D.; Anderson, R. T.; Lovley, D. R. *Appl. Environ. Microbiol.* **1996**, *62*, 1099.

(10) Coates, J. D.; Anderson, R. T.; Woodward, J. C.; Phillips, E. J. P.; et al. *Environ. Sci. Technol.* **1996**, *30*, 2784.
(11) Coats, J. D.; Woodward, J. C.; Allen, J.; Philp, P.; et al. *Appl. Environ. Microbiol.* **1997**, *63*, 3589.
(12) Bauer, J. E.; Capone, D. G. *Appl. Environ. Microbiol.* **1988**, *54*, 1649.
(13) Grosser, R. J.; Warshawsky, D.; Vestal J. R. *Environ. Toxicol. Chem.* **1995**, *14*, 375.
(14) Grosser, R. J.; Warshawsky, D.; Vestal, J. R. *Environ. Toxicol. Chem.* **1991**, *57*, 3462.
(15) Efroymson, R. A.; Alexander, M. *Environ. Sci. Technol.* **1995**, *29*, 515.
(16) Hatzinger, P. B.; Alexander, M. *Environ. Sci. Technol.* **1995**, *29*, 537.
(17) Guerin, W. F.; Boyd, S. A. *Appl. Environ. Microbiol.* **1992**, *58*, 1142.
(18) Genthner, B. R. S.; Townsene, G. T.; Lantz, S. E.; Mueller, J. G. *Arch Environ. Contam. Toxicol.* **1997**, *32*, 99.
(19) Hurst, C. J.; Sims, R. C.; Sims, J. L.; Sorensen, D. L.; McLean, J. E.; Huling, S. *J. Hazard. Materials* **1996**, *51*, 193.
(20) Kaestner, M.; Mahro, B. *Appl. Microbiol. Biotechnol.* **1996**, *44*, 668.
(21) Karimi-Lotfabad, S.; Pickard, M. A.; Gray, M. R. *Environ. Sci. Technol.* **1996**, *30*, 1145.
(22) Comerford, N. B.; Jerez, A.; Freitas, A. A.; Montgomery, J. *Soil Science* **1996**, *161*, 194.
(23) Haraguchi, A. *Wetland* **1995**, *15*, 242.
(24) Singleton, P. L. *Austr. J. Soil Research* **1991**, *29*, 467.
(25) Malkomes, H. P. *Z. Pflanzenernaehr. Bodenk.* **1991**, *154*, 325.
(26) Sarig, S.; Steinberger, Y. *Geoderma* **1993**, *56*, 599.
(27) Fliessbach, A.; Sarig, S.; Steinberger, Y. *Arid Soil Res. Rehab.* **1994**, *8*, 353.
(28) Steinberger, Y.; Sarig, S. *Bio. Fertility Soils* **1993**, *16*, 188.
(29) Bramley, R. G. V.; White, R. E. *Austr. J. Soil Res.* **1989**, *27*, 711.
(30) Harris, R. F. In *Water Potential in Soil Microbiology*; Parr, L. F., Gardner, W. R., Elliott, L. F., Eds.; SSSA: Madison, WI, 1981; pp 23−96.
(31) Voudrias, E. A.; Yeh, M. F. *Ground Water* **1994**, *32*, 305.
(32) Rainwater, K.; Mayfield, M. P.; Heintz, C. E.; Claborn, B. J. In *Biological Processes: Innovative Hazardous Waste Treatment Technology Series*; Freeman, H. M., Sferra, P. R., Eds.; Technomic: Cincinnati, OH, 1991; Vol. 3; pp 123−130.
(33) Mackay, D.; Shiu, W. Y.; Ma, K. C. *Handbook of Physical-Chemical Properties and Environmental Fate for Organic Chemicals*; Lewis Publishers: MI, 1992; Vol. II, Chapter 2.
(34) Dolan, M. E.; McCarty, P. L. Environ. Sci. Technol. **1995**, *29*, 1892.
(35) Holman, H. Y.; Tsang, W. Y. In *In Situ Aeration: Air Sparging, Bioventing and Related Remediation Processes*; Hinchee, R. E., Miller, R. N., Johnson, P. C., Eds.; Battelle Press: Columbus, OH, 1995; pp 323−332.
(36) Nielsen, P. H.; Christensen, T. H. *J. Contam. Hydrol.* **1994**, *15*, 305.
(37) Gatti, R. C. Lawrence Berkeley National Laboratory, personal communication, 1996.
(38) Bjerg, P. L.; Brun, A.; Nielsen, P. H.; Christensen, T. H. *Water Resour. Res.* **1996**, *32*, 1831.
(39) Madsen, E. L.; Mann, C. L.; Bilotta, S. E. *Environ. Toxicol. Chem.* **1996**, *15*, 1876.
(40) Pinelli, D.; Fava, F.; Nocentini, M.; Pasquali, G. *J. Soil Contam.* **1997**, *6*, 243.
(41) Cheney, M. A.; McGrath, A.; Sposito, G.; Criddle, R. *Abstracts of Papers*; American Chemical Society: Washington, DC, **1995**; Vol. 209, p 1.
(42) Ahn, I. S.; Lion, L. W.; Shuler, M. L. *Biotechnol. Bioeng.* **1996**, *51*, 1.
(43) Bosma, T. N. P.; Middeldorp, P. J. M.; Shraa, G.; Zehnder, A. J. B. *Environ. Sci. Technol.* **1997**, *31*, 248.
(44) Wu, S. C.; Gschwend, P. M. *Environ. Sci. Technol.* **1986**, *20*, 717.
(45) Holmén, B. T.; Gschwend, P. M. *Environ. Sci. Technol.* **1997**, *31*, 105.
(46) Agathos, S. N.; Hellin, E.; Ali-Khodja, H. et al. *Biodegradation* **1997**, *6*, 251.
(47) Kirchner, K.; Wagner, S.; Rehm, H. J. *Appl. Microbiol. Biotechnol.* **1996**, *45*, 415.
(48) Reviewer no. 1 communication, 1998.
(49) Ahn, I.-S.; Ghiorse, W. C.; Lion, L. W.; Shuler, M. L. *Biotechnol. Bioeng.* **1998**, *59*, 587.

Received for review July 10, 1998. Revised manuscript received March 9, 1999. Accepted March 12, 1999.

ES980701K